The behavior of the three-term method shown in Fig. 3 is explained as follows. Returning to Eq. (1), there is the numerical possibility that a steady state can be achieved where $(\partial g/\partial t)_t$ and $(\partial^2 g/\partial t^2)_t$ do not approach zero, but rather the first-and second-order terms in Eq. (1) eventually become of equal magnitude and opposite in sign, hence cancelling and resulting in a stationary value for g from one time step to the next. In previous applications of the time-dependent method employing Eq. (1),[1,4,5,6,7] this behavior was not observed; in all cases, both time derivatives in Eq. (1) became very small as the steady state was approached. However, occasionally the aforementioned anomalous behavior can occur in practice, and such a case is illustrated in Fig. 3. Such remote anomalies do not occur with the present two-term method.

In conclusion, the two-term and three-term methods yield essentially identical steady-state results for nonequilibrium nozzle flows. However, the two-term method [Eq. (2)] discussed in the present Note must be considered superior because it requires less algebra, it requires fewer computations, hence less computer time, and the time derivatives rapidly approach zero in all situations. Hence, the already straightforward and simple analysis of nonequilibrium nozzle flows described in Ref. 1 is made even simpler by the present modification.

References

[1] Anderson, J. D., Jr., "A Time-Dependent Analysis for Vibrational and Chemical Nonequilibrium Nozzle Flows," *AIAA Journal*, Vol. 8, No. 3, March 1970, pp. 545–550.

[2] MacCormack, R. W., "The Effect of Viscosity in Hypervelocity Impact Cratering," AIAA Paper 69-354, Cincinnati, Ohio, 1969.

[3] Anderson, J. D., Jr., "Numerical Experiments Associated with Gas Dynamic Lasers," NOLTR 70-198, Sept. 1970.

[4] Anderson, J. D., Jr., "Time-Dependent Analysis of Population Inversions in an Expanding Gas," *The Physics of Fluids*, Vol. 13, No. 8, Aug. 1970, pp. 1983–1989.

[5] Anderson, J. D., Jr., "A Time-Dependent Quasi-One-Dimensional Analysis of Population Inversions in an Expanding Gas," NOLTR 69-200, Dec. 1969, U. S. Naval Ordnance Lab., White Oak, Md.

[6] Anderson, J. D., Jr., Albacete, L. M., and Winkelmann, A. E., "On Hypersonic Blunt Body Flow Fields Obtained with a Time-Dependent Technique," NOLTR 68-129, Aug. 1968, U. S. Naval Ordance Lab., White Oak, Md.

[7] Anderson, J. D., Jr., "A Time-Dependent Analysis for Quasi-One-Dimensional Nozzle Flows with Vibrational and Chemical Nonequilibrium," NOLTR 69-52, May 1969, U. S. Naval Ordnance Lab., White Oak, Md.

A Direction-Indicating Color Schlieren System

GARY S. SETTLES*

University of Tennessee, Knoxville, Tenn.

THE conventional black-and-white Toepler schlieren system[1,2] displays only those refractive index gradients which deflect light normal to its knife-edge. Other monochrome schlieren methods have been developed to overcome this disadvantage,[3,4] but these methods have limited utility as a result of difficulties with loss of information on gradient directions, separate images, and the compromise between sensitivity and image resolution.

Received August 19, 1970.

* Undergraduate Student, Mechanical and Aerospace Engineering Department. Student Member AIAA.

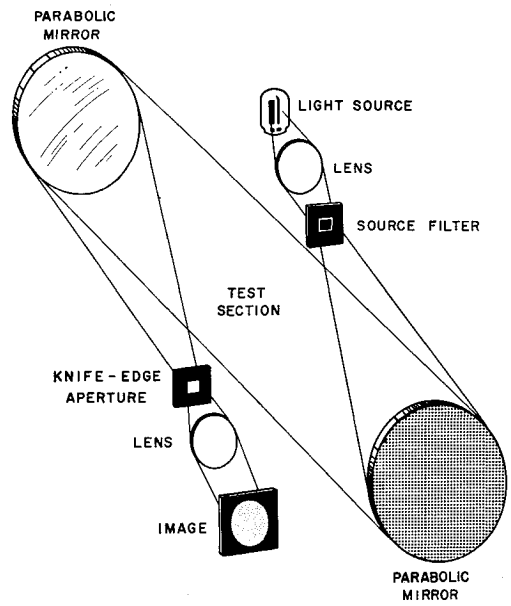

Fig. 1 Arrangement of direction-indicating color schlieren system.

The new color schlieren system described in this Note produces a single image, in which refractive index gradients n all radial directions are displayed and directionally color-coded. In addition, this schlieren system has sensitivity and resolution capabilities comparable to those of the single knife-edge monochrome schlieren, and uses essentially the same optical components as the monochrome schlieren.

A diagram of the new color schlieren system is shown in Fig. 1. The system consists of a white light source, a lens, a color source filter arrangement, two parabolic mirrors, a knife-edge aperture, and a camera lens and screen. These components are arranged in the standard Z-type schlieren configuration.

The source filter, which is illustrated in Fig. 2, breaks the schlieren light beam up into four color bands, which are arranged in a square. The beam proceeds from the source filter to the first parabolic mirror, where it is collimated. The collimated beam passes through the test section and is refocussed by the second parabolic mirror to form an image of the color source bands at the knife-edge location. A square knife-edge aperture cuts off about half of the light of each color, but allows the remaining light to form a schlieren image on the screen.

In going from the source filter to the first parabolic mirror, light of the four colors overlaps and mixes to form a beam of

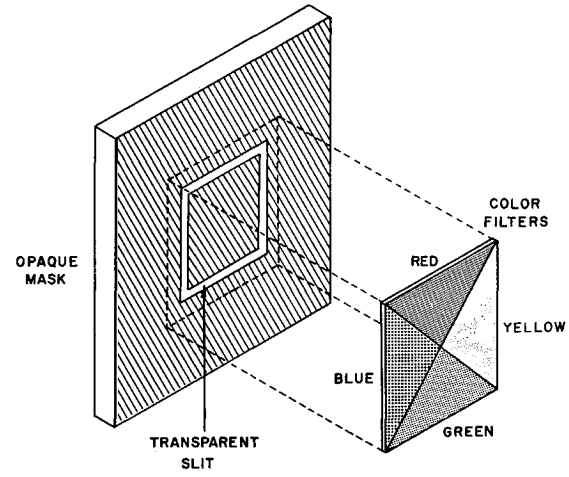

Fig. 2 Source filter assembly.

a single hue. Since the schlieren image is focussed on the test section plane, it is evenly illuminated by light of this hue when there are no refractive index gradients in the test section. If a local gradient is introduced in the test section, it refracts some of the light, which is a mixture of the four colors, and causes a weak image of the color source filter bands to undergo a displacement in the knife-edge plane. Some of the color bands of this weak source filter image will be completely blocked off, while others will pass through the knife-edge aperture and cause a local color shift in the schlieren image. The configuration of the gradient in the test section determines the shape and location of this color shift, and the direction of the gradient determines which color combination passes through the aperture to illuminate a local region of the schlieren image. This arrangement provides a discrete color code in the schlieren image for each different gradient angle, as illustrated in Fig. 3.

The color filter arrangement shown in Fig. 2 has yielded the most successful results to date. It produces a uniform color-coding spectrum by taking advantage of the fact that colored light from adjacent bands in the source filter can mix in the schlieren image, but colors from opposite bands can only replace each other in the image. With other color filter combinations, care must be taken to prevent the appearance of ambiguous hues or white light in the schlieren image as a result of incorrect arrangement of the color filters.

The background in the image produced by the direction-indicating color schlieren system may be unevenly illuminated due to the effects of astigmatism.[2] These effects can be alleviated by the method proposed by Prescott and Gayhart,[5] or by using separate horizontal and vertical slits rather than a single knife-edge aperture.

Cords[6] has shown that apertures in the schlieren knife-edge plane must not be made too small if diffraction effects resulting in a loss of image resolution are to be avoided. His method of minimizing the effects of the usual sensitivity-resolution compromise is employed in the new color schlieren system described in this Note. The new system attains high sensitivity when the widths of the slits in the source filter are very small. The lengths of these slits, however, and not their widths, determine the size of the knife-edge aperture, so that the aperture may be made large enough to avoid any loss of image resolution as a result of diffraction effects.

A comparison in monochrome of the image resolution and sensitivity of horizontal and vertical knife-edge black-and-white schlieren with that of the new color schlieren system is shown in Fig. 4. Note that the boundary layers on model and wind-tunnel walls do not appear in the vertical knife-edge photo, while in the horizontal knife-edge image, the boundary layer on the lower surface of the model obscures

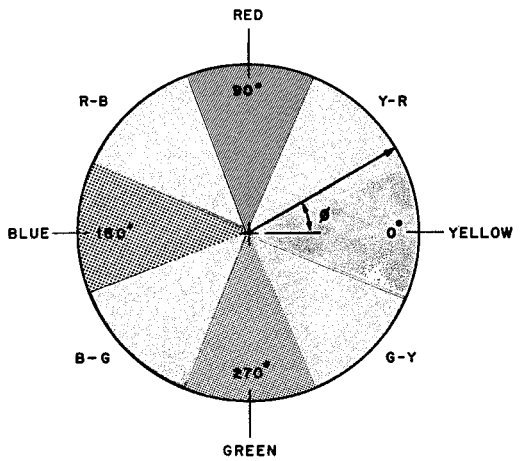

Fig. 3 Diagram correlating image color with gradient angle, ϕ.

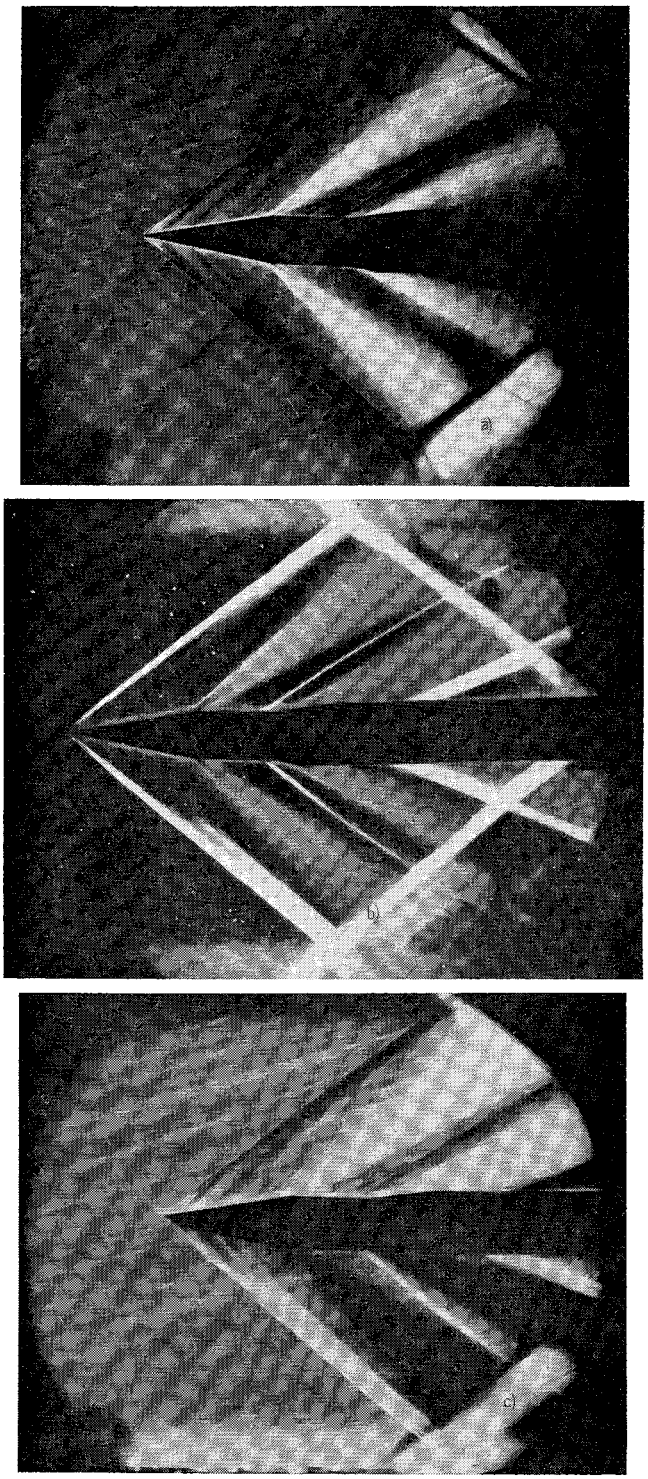

Fig. 4 Mach 2 airflow over a wedge model as photographed by: a) vertical knife-edge monochrome schlieren; b) direction-indicating color schlieren; and c) horizontal knife-edge monochrome schlieren.

the outline of the model. These disadvantages are not present in the photo made with the new color schlieren system, since it displays patterns characteristic of both knife-edge orientations in a single image, and since the use of color yields good contrast between model and flowfield. Other advantages of the use of color[2] in this new system are 1) an added sensitivity effect, and 2) the enhanced general and scientific appeal of a color presentation. The monochrome illustration of Fig. 4 does not demonstrate the major advantage of the new schlieren system, which is its directional color-coding ability.

References

[1] Toepler, A., "Beobachtungen nach einer Neuen Optischen Methode," *Poggendorf's Annalen der Physik und Chemie*, Vol. 127, No. 4, May 1866, pp. 556–580.

[2] Holder, D. W. and North, R. J., "Schlieren Methods," NPL Notes on Applied Science No. 31, Her Majesty's Stationery Office, London, 1963.

[3] Edmondson, R. B., Gayhart, E. L., and Olsen, H. L., "Radial Symmetry in a Schlieren Image," *Journal of the Optical Society of America*, Vol. 42, No. 12, Dec. 1952, p. 984.

[4] Barry, F. W. and Edelman, G. M., "An Improved Schlieren Apparatus," *Journal of the Aeronautical Sciences*, Vol. 15, No. 6, June 1948, p. 364.

[5] Prescott, R. and Gayhart, E. L., "A Method of Correction of Astigmatism in Schlieren Systems," *Journal of the Aeronautical Sciences*, Vol. 18, No. 1, Jan. 1951, p. 69.

[6] Cords, P. H., Jr., "A High Resolution, High Sensitivity Color Schlieren Method," *Society of Photo-Optical Instrumentation Engineers Journal*, Vol. 6, No. 3, Feb.-March 1968, pp. 85–88.

A Modified Form of the Coles Compressibility Transformation

CONSTANTINO ECONOMOS*
General Applied Science Laboratories, Inc., Westbury, N. Y.

Nomenclature

$c_f,\bar{c}_f$ = local skin-friction coefficients
F = nondimensional transpiration rate $= \rho_w v_w/\rho_e u_e$
I = integral defined by [Eq. (7)]
$R_y,R_{\bar{y}}$ = Reynolds number based on normal coordinates
$R_\delta,R_{\bar{\delta}}$ = Reynolds number based on boundary-layer thicknesses
$R_\theta,R_{\bar{\theta}}$ = Reynolds number based on momentum thicknesses
$u,\bar{u}$ = streamwise velocity components
$v,\bar{v}$ = normal velocity components
$x,\bar{x}$ = streamwise coordinates
$y,\bar{y}$ = normal coordinates
α = $R_{\bar{y}}/R_{\bar{\delta}}$
η,κ,ξ,σ = scaling parameters of the transformation
$\tau,\bar{\tau}$ = shear stresses
$\mu,\bar{\mu}$ = coefficients of laminar viscosity
Π = Coles wake parameter
$\rho,\bar{\rho}$ = densities
$\tilde{\sigma}$ = $\sigma\mu_e/\bar{\mu}$
$\psi,\bar{\psi}$ = stream functions:
$\partial\psi/\partial y = \rho u;\ \partial\psi/\partial x = \rho_w v_w - \rho v$
$\partial\bar{\psi}/\partial\bar{y} = \bar{\rho}\bar{u};\ \partial\bar{\psi}/\partial\bar{x} = \bar{\rho}\bar{v}_w - \bar{\rho}\bar{v}$

Subscripts

e = conditions external to boundary layer
w = conditions at the wall
$(\ )$ = variables of the *VP* flow
$(\bar{\ })$ = variables of the *CP* flow
$(\tilde{\ })$ = normalization with respect to corresponding external value; e.g., $\tilde{u} = u/u_e$

Introduction

NUMEROUS investigators[1,2] have analyzed velocity profiles obtained in high-speed flows over impermeable flat plates by means of the Coles compressibility transformation.[3] In all cases it was found that the velocity defect portion of the transformed profiles was not well correlated in the sense that the flat plate value of the Coles wake parameter Π was not recovered. A similar result was also observed for the case of low-speed flow with foreign gas injection.[4] These effects are demonstrated by some representative results presented in Fig. 1.

It has been suggested[5,6] that this behavior may be caused by the use of a Howarth-Dorodnytsin (HD) scaling throughout the boundary layer and that such use may not be appropriate in the wake region. The purpose of this Note is to outline a modification of the original transformation which permits suppression of the HD scaling, while retaining certain other useful features of the transformation; e.g., detailed mapping of the "law of the wall" region.

Modified Transformation

The modification introduces a new parameter $\kappa(y)$, such that the y stretching takes the form

$$(\bar{\rho}/\rho)(\partial\bar{y}/\partial y)_x = \eta(x)\kappa(y) \tag{1}$$

In order to preserve the original correspondence between the axial velocity components given by $u/u_e = \bar{u}/\bar{u}_e \equiv \tilde{u}$, it is also necessary to modify the corresponding stretching for the stream function according to†

$$(\partial\bar{\psi}/\partial\psi)_x = \sigma(x)\kappa(y) \tag{2}$$

The development from this point follows that of Coles.[3] In particular, with the axial coordinates related by $d\bar{x}/dx = \xi(x)$, the correspondence between velocity components becomes‡

$$u = (\eta/\sigma)\tilde{u} \tag{3}$$

$$\rho v = (1/\sigma\kappa)[\bar{\rho}\bar{v}\xi - \bar{\rho}\bar{u}(\partial\bar{y}/\partial x)_y + (\partial\bar{\psi}/\partial x)_\psi] \tag{4}$$

while the convective term appearing in the x-wise momentum equation transforms according to

$$\rho u\partial u/\partial x + \rho v\partial u/\partial y = (\bar{\rho}\bar{u}\partial\bar{u}/\partial\bar{x} + \bar{\rho}\bar{v}\partial\bar{u}/\partial\bar{y}) \times (\rho\xi\eta^2/\bar{\rho}\sigma^2) + (\rho\eta^2/\bar{\rho}\sigma^2)(\partial\bar{u}/\partial\bar{y})(\partial\bar{\psi}/\partial x)_\psi \tag{5}$$

where, by virtue of Eq. (3), we have taken $\eta/\sigma = u_e/\bar{u}_e = \text{const}$. Evidently, the first of these terms provides the desired transport term corresponding to the constant property (CP) flowfield, so that, in principle, transformation of the differential equations describing the variable property (VP) flow to a CP form can be completed by suitably combining the second term with the shear derivatives $\partial\tau/\partial y$ and

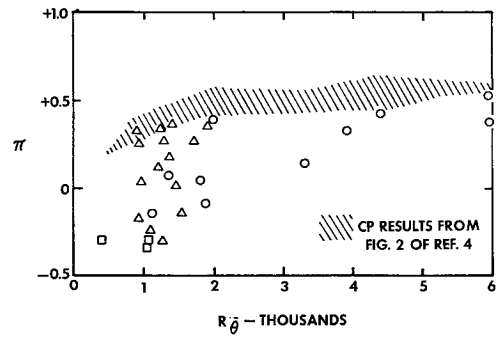

Fig. 1 Magnitude of wake component found in several VP boundary-layer configurations transformed according to the Coles stretching: triangles, low-speed helium injection results[7]; circles, adiabatic impermeable results[8]; squares, impermeable results with heat transfer.[9]

Received May 11, 1970; revision received August 12, 1970. The author is pleased to acknowledge Dr. P. A. Libby of USC, San Diego for suggesting this investigation.

* Supervisor, Thermochemistry and Viscous Flow Section. Member AIAA.

† In view of the manner in which the stream function has been defined here, the earlier modification proposed in Ref. 4, to account properly for wall mass transfer, is included herein.

‡ The development from this point is specialized to the case of zero mass transfer and zero pressure gradient in both flows; extension to these more general cases is straightforward but is not included here for the sake of brevity.